JMEPEG (2008) 17:271–279
DOI: 10.1007/s11665-007-9140-1

1059-9495/$19.00

Studies on Production and Thermo-Mechanical Treatment of 0.32% Nitrogen Alloyed Duplex Stainless Steel

P. Chandramohan, S.S. Mohamed Nazirudeen, and S.S. Ramakrishnan

(Submitted April 19, 2006; in revised form May 5, 2007)

Duplex stainless steel with nitrogen content 0.32% was produced using a conventional induction furnace under normal ambient atmosphere. The samples were subsequently hot forged to various size reductions (23-57%). Both the as-cast and the hot-forged samples were examined for changes in the microstructure and mechanical properties. The results reveal that the optimal-mechanical properties were noticed for a forging deformation of 48%. Texture analysis was carried out in these samples using Inverse Pole Figures (IPF) and Orientation Distribution Function (ODF). However, IPF and ODF results revealed that bulk texture was weak after hot forging.

Keywords austenite, duplex stainless steel, ferrite, forging, texture

1. Introduction

Duplex stainless steel (DSS) belongs to the family of stainless steels which contain two phases, i.e., ferrite and austenite in almost equal proportions. The ''Duplex'' microstructure is obtained by controlled alloying with nitrogen, nickel (austenite stabilizer), and chromium (ferrite stabilizer). Small percentages of Mo, Mn, Si, and other alloying elements are also present in these alloys (Ref 1).

One of the most common failure mechanisms in stainless steel is chloride-induced Stress Corrosion Cracking (SCC). The conventional austenitic grades are particularly susceptible to this failure mode. However, Duplex stainless steels offer significant resistance to this form of cracking (Ref 2-4). In addition to, they have better corrosion resistance in severe chloride atmosphere besides better mechanical properties.

In the early stages, the commercial products in duplex stainless steels were developed using nickel as the austenite stabilizer. Subsequently, nickel was found to be expensive and allergy causing and was partially replaced by nitrogen.

Nitrogen bearing duplex stainless steels were manufactured by various controlled atmospheric techniques (Ref 5-8). The production of nitrogen alloyed DSS in a conventional furnace under normal atmospheric condition was also reported in the literature as this meets the competitive requirement of low-cost manufacture without sophisticated equipment and controls (Ref 9).

P. Chandramohan, Sri Krishna College of Engg and Tech, Coimbatore 641 008, India; and **S.S. Mohamed Nazirudeen,** PSG College of Technology, Coimbatore 641004, India; and **S.S. Ramakrishnan,** TamilNadu College of Engineering, Coimbatore 641004, India. Contact e-mail: pcmohu@yahoo.co.in.

Thermo-mechanical treatment is expected to improve the mechanical properties of DSS. In these alloys, hot deformation was done in the temperature range of 1000-1300 °C followed by solution annealing and quenching (Ref 10). After hot-forging DSS, solutionizing is followed by water quenching to avoid precipitation (Ref 11). A study on 22 Cr DSS reveals the fact that it should not be hot worked at temperature above 1200 °C, in order to avoid the transformation of austenite to ferrite (Ref 12). The higher the deformation temperature, the greater is the probability for the formation of ferrite from austenite especially in specimens containing less than 2% nitrogen (Ref 13, 14).

It is a proven fact that, texturing influences the properties of the mechanically worked material to a remarkable extent. The extent of texture development caused by treatments like rolling and extrusion in various steels, aluminum alloys, and Zr-Nb alloys has been studied by several researchers (Ref 15, 16). The general inference is that cold rolling is insignificant in two-phase alloys, but very noticeable in single-phase alloys.

The authors felt that the study of texture development caused by hot-forging DSS was rarely reported in the literature, and hence this work was attempted using Inverse Pole Figure (IPF) and Orientation Distribution Function (ODF).

Duplex stainless steel alloys with 0.15 and 0.23% N had been produced in a conventional induction furnace under atmospheric pressure and subjected to various solution treatment temperatures ranging from 1010 to 1140 °C. But, better mechanical properties were observed at the solution treatment temperature of 1060 °C by Chandramohan et al. (Ref 9). The higher the nitrogen content (0.23% compared to 0.15%), the better were the mechanical properties. It was therefore expected that, by increasing the nitrogen content to 0.32% would very likely increase the mechanical properties further.

The scope of the present work is therefore

(i) To produce DSS with higher nitrogen content (0.32% N) followed by heat treatment and hot forging.
(ii) To study the effects of hot forging on microstructure, mechanical properties, and bulk texture.

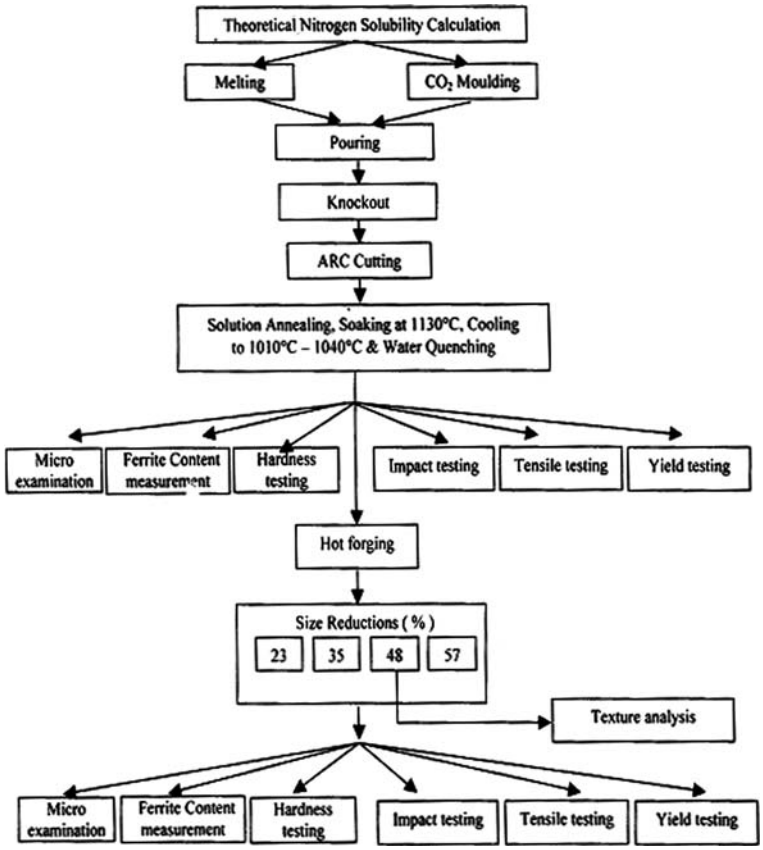

Fig. 1 Flowchart

2. Experimental Work

The flowchart in Fig. 1 shows the production sequence of the alloy (DSS with 0.32% N) and the subsequent experimental work carried out on this alloy.

The theoretical solubility of nitrogen in the iron was calculated to be 0.23% using Sieverts' law. The solubility of nitrogen at 1600 °C in the Duplex stainless steel containing Cr, Ni, Mn, Mo, N, Si, C is given as K/f_N^x, where reaction constant K is 0.045 and partial pressure $P_{N_2} = 1$ bar, and f_N^x is calculated using the Eq 1

$$\begin{aligned}\text{Log } f_N^x = {} & e_N^N\%N + e_N^{Cr} + r_N^{Cr}(\%Cr)^2 + e_N^{Mn}\%Mn + r_N^{Mn}(\%Mn)^2 \\ & + e_N^{Mo}\%Mo + r_N^{Mo}(\%Mo)^2 + e_N^{Ni}\%Ni + r_N^{Ni}(\%Ni)^2 \\ & + e_N^V\%Si + r_N^V(\%Si)^2 + e_N^C\%C + r_N^C(\%C)^2. \end{aligned} \quad \text{(Eq 1)}$$

where e_N refers to first order parameter and r_N refers to the second-order parameter.

2.1 Melting and Chemical Analysis

The alloy with the nominal nitrogen content of 0.32% N was melted in a high-frequency induction furnace, after adding the raw materials as per the charge calculation given in Table 1. Pure iron, Low-carbon stainless scrap, and Low-carbon ferro chromium were charged in the same sequence. After the melting of the charge, low-carbon ferro manganese, ferro silicon, and Nitrogen alloyed low-carbon Ferro chromium were added to the molten metal at 1400 °C. Then degassing was done by purging argon gas through 316 L stainless steel tube, followed by tapping at 1550 °C into the laddle in which the deoxidizers were added. As per the Fe Cr Ni phase diagram in Fig. 2, the melting point of 25% Cr-6% Ni alloyed duplex stainless steel is close to 1480 °C and hence a slightly higher temperature of 1550 °C was selected as the tapping temperature (Ref 1).

The molten metal was poured into CO_2 molds for Y block castings as per ASTM A 370 specifications. The CO_2 molds poured were allowed to cool for 6 h and knocked out manually. The chemical composition of the alloy was analyzed using spectrovac (Table 2).

2.2 Heat Treatment and Testing

All the Y block castings of the DSS alloy with 0.32% N were solution annealed at 1130 °C, furnace cooled to 1040 °C, and then water quenched. The purpose of the above-mentioned treatment is to achieve a homogeneous heat distribution in the specimen without intermetallic phases. The solution annealing temperature of 1130 °C was selected based on the Fe Cr Ni phase diagram (Ref 1). Heat-treated specimens of the alloy were studied for Ferrite volume fraction and mechanical properties like hardness, impact strength, yield strength, and tensile strength.

2.3 Hot Forging

Cast- and heat-treated samples of the alloy were heated to 1100 °C using an oil-fired furnace of 100 kg capacity which

Table 1 Charge material composition and calculation

Charge	%C	%Fe	%Ni	%Cr	%MO	%Mn	%N	
Charge material composition								
Pure iron	0.010	99.9						
Pure nickel	0.015		99					
LC Fe-Cr	0.020			60.5				
LC Fe-Mo	0.020				60.0			
LC Fe-Mn	0.08					58		
N Fe Cr	0.03			55			6	
Charge	Weight	%Ca	%Si	%Ti	%Zr	%Se	%Fe	%C
Deoxidizers in laddle								
CaSi	0.1	32	61				Remaining	0.05
FeTi	0.1			35			Remaining	0.1
FeSiZr	0.1		18		35		Remaining	0.05
Se	0.05					99	Remaining	
Charge	Wt, kg	C, kg	Fe, kg	Ni, kg	Cr, kg	MO, kg	Mn, kg	N, kg
Charge calculation								
Pure iron	44.0	0.0044	44.0					
Pure Ni	6.56	0.00098	0.06	6.5				
LC FeCr	36.0	0.0072	14.2		21.8			
LCFeMo	6.66	0.0013	2.66			4.0		
LCFeMn	0.862	0.0007	0.36				0.5	
NFeCr	5.83	0.0017	0.36		3.20			0.35
Total	100	0.0163	61.60	6.5	25.0	4.0	0.5	0.35
Pouring temperature = 1540 °C								

Table 2 Chemical composition of the alloy

Alloy	%C	%Si	%Mn	%P	%S	%Cr	%Ni	%MO	%N	%V	%Nb
DSS alloy with 0.32% N	0.0245	0.8819	0.4054	0.020	0.009	24.45	6.29	4.197	0.324	0.056	0.0117

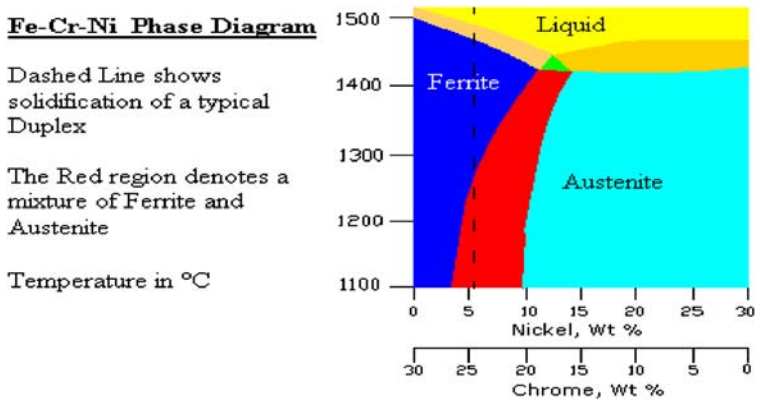

Fig. 2 Fe Cr Ni phase diagram

uses a 2-HP blower. Three thermocouples were located on three walls of the furnace, packed with firebrick and fireclay. The heated samples were taken out one by one, and subjected to upset-forging in a pneumatic press. The samples were hot forged and the thickness is reduced from 30 mm. The percentage size reductions were 23, 35, 48, and 57 in different specimens.

2.4 Texture Study

The texture studies were carried out using x-ray Diffractometer, in order to study the effect of anisotropy on mechanical properties of the material such as hardness and strength. Inverse Pole Figure (IPF) was constructed by drawing unit triangle [001], [011] and [111]. IPF indicates how intensely each crystallographic direction is oriented parallel to the external reference direction viz., axis of the forged specimen. Inverse Pole Figure at best gives only a rough estimate of texturing, but not any information about crystallographic direction. In order to obtain quantitative information on the volume fraction of different texture components, ODF was constructed in the form of a two-dimensional diagram showing the relationship of two Euler angles ϕ_1 and ϕ with the other Euler angle ϕ_2.

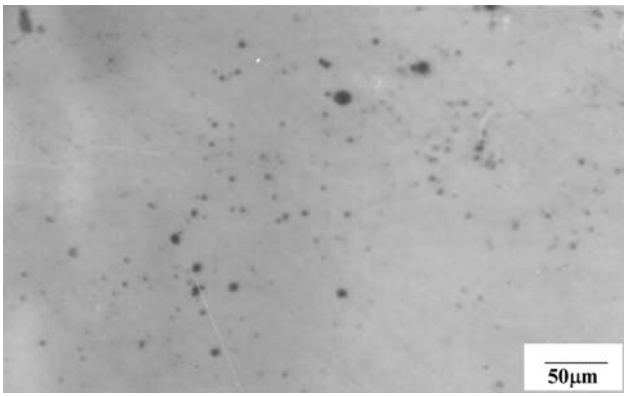

Fig. 3 Optical micrograph of DSS alloy with 0.32% N, containing micro porosities

3. Results and Discussions

3.1 Theoretical Nitrogen Solubility

The calculated theoretical nitrogen solubility was 0.23%, whereas the actual nitrogen content achieved in the alloy was 0.32%. This difference results in the occurrence of tiny gas porosities, observed on the surface of the castings as shown in the micro structural photograph (Fig. 3). This is in agreement with the findings of Young Hwan Park and Zin-Hyoung Lee (2001), who also had observed gas porosities with increasing nitrogen content in Duplex stainless steels.

3.2 Cast- and Heat-treated DSS Alloy

3.2.1 Mechanical Properties. The hardness values (6 readings per specimen) of the cast and solutionized specimens tested at 10 kg load and at 100 g load are listed in Table 3. By applying a micro hardness load of 100 g, hardness values of the individual phases (i.e., ferrite and austenite) are measured. The micro hardness of the ferrite phase is lower than the austenite phase. The overall hardness, however, shows a lower value than micro hardness values of either phase. This is in agreement with the findings of various researchers (Ref 17-19) in the case of nitrogen alloyed Duplex stainless steels. The hardness of austenite ranges between 150 and 210 VHN and ferrite from 150 to 180 VHN in the normal stainless steel without nitrogen. But in Duplex Stainless Steels, the hardness is always higher because of the presence of nitrogen. The increase in the hardness of duplex structure is due to various strengthening mechanisms (e.g.,): Austenite particles in the ferrite matrix constraining the movement of ferrite grain boundaries; Interstitial solid solution hardening (N); Substitutional solid solution hardening (Cr, Mo, Ni, etc.); Strengthening by grain refinement due to the presence of two phases; Short range atomic ordering of N and lesser stacking fault energy of austenite, retarding dislocation climb between slip planes; and the strain induced by differential contraction of the two phases on cooling from annealing temperatures (Ref 20, 21).

As the nitrogen content increases from 0.15 to 0.23% in DSS, an increase in hardness is observed (Ref 9). However, in the DSS alloy with 0.32% N, the overall hardness is lower than in DSS alloy with 0.23%, in spite of its higher-nitrogen content along with more austenite content.

The impact toughness values of alloy with 0.15 and 0.23% N ranges from 106 to 134 J, respectively, at room temperature

Table 3 Mechanical properties of cast and solutionized specimens

Mechanical properties	Alloy with 0.15% N	Alloy with 0.23% N	Alloy with 0.32% N
Hardness at 10 kg load (VHN)	252-260	281-300	255-266
Hardness at 100 g load (VHN)			
Ferrite	315	355	320
Austenite	324	358	332
Impact toughness (J)			
At Room temp.	106	134	114
At –40 °C	63	76	54
Ultimate tensile strength (MPa)	755	816	789
Yield strength (MPa)	560	568	597
% Elongation	35	38	30

Table 4 Properties of forged-DSS specimen with 0.32% N

	Size reduction, %				
Properties	**0**	**23**	**35**	**48**	**57**
Ferrite volume	43	47	58	42	50
Hardness at 10 kg load (VHN)	255-266	294	287	294	274
Hardness at 100 g load (VHN)					
Ferrite	320	339	382	413	375
Austenite	332	497	439	424	377
Impact toughness (J)					
At Room temp.	114	91	96	105	88
At –40 °C	54	81	82	85	75
Ultimate tensile strength (MPa)	789	894	913	941	943
Yield strength (MPa)	597	549	542	581	574

(Table 4). Austenite content of the DSS alloys with 0.15 and 0.23% N is 45 and 53% (Ref 9). Eventhough alloy 3 (0.32% N) contains a higher-austenite content (57%) its mechanical properties like hardness, impact toughness, and ultimate tensile strength are less than that of the alloys with 0.15 and 0.23% N. This is due to the presence of micro porosities. Hence, the samples are hot forged to find out possible improvement in the mechanical properties with increase in nitrogen content (eliminating the micro porosity effect by hot forging).

3.3 Hot Forging

3.3.1 Micro Structural Study. With the increase in size reduction of the alloy from 23 to 57%, ferrite volume fraction ranges from 42% to a maximum of 58%. The ferrite content of the alloy specimen before hot forging is 43%. After hot forging, the ferrite content is more than 43% in all the size reductions (Table 4).

The process of hot forging increases the transformation of austenite to ferrite. This phenomenon of ''deformation-induced ferrite'' might be due to the fact that the deformation induces more substructure in α (BCC) phase as compared to γ (FCC) phase. Lesser tendency for substructure formation in FCC is due to the lower stacking fault energy of FCC. The nucleation mechanism of γ phase formation (FCC) is by the phase boundary bulging and migration in single-phase alloys. However, in dual phase alloys, phase boundary bulging is restricted by the second phase and hence the possible nucleation is only

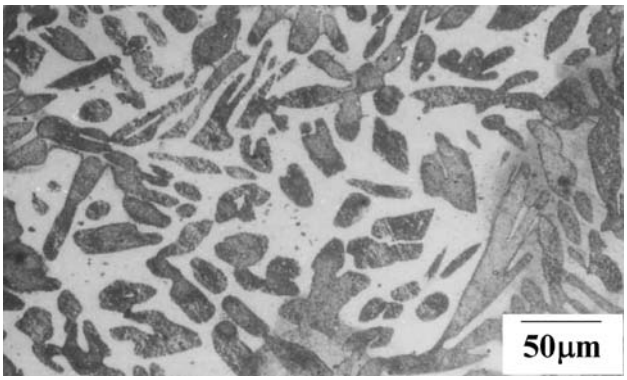

Fig. 4 Optical micrograph of alloy with 0.32% N—cast and solutionized

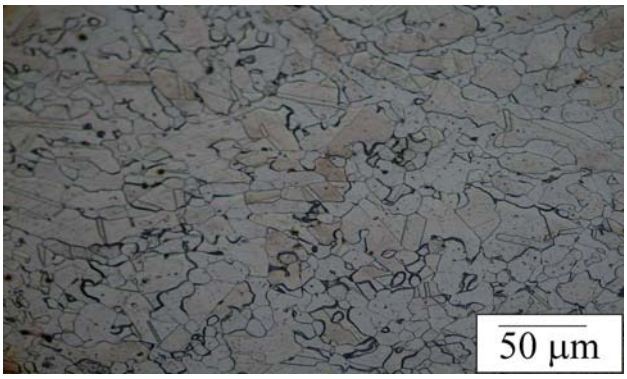

Fig. 5 Optical micrograph of alloy with 0.32% N—hot forged

by coalescence of sub grains. The deformation does not create more sub grains in γ as compared to α phase. So the relative volume fraction of γ as compared to α is less in forged DSS than in cast DSS, because of the effect of plastic deformation (Ref 22, 23). This explains the reason for higher-ferrite content in these specimens.

Microstructures of specimens, before and after hot forging, are shown in Fig. 4 and 5, respectively. Hot forging did not result in grain elongation or grain coarsening. In fact, some of the grains appear as refined and partially equiaxed. In order to study the effect of hot forging on grain refinement, the number of grains are counted as per ASTM E 112-63 standards, and the results are shown in Fig. 6. The results reveal that increasing size reduction refines the grain size. The maximum increase in the number of grain is observed in specimens of 48% size reduction.

3.3.2 Effect of Hot Forging on Hardness. The hardness values of various samples were determined with loads of both 10 kg and 100 g. The results are given in Table 4. Six readings were taken at different locations and the average was considered for the analysis. The results reveal that the hardness values determined at 10 kg load in the as-cast (unforged) specimen ranges from 255 to 266 VHN, whereas in hot-forged specimens hardness values are higher. The maximum hardness value was observed with size reduction of 48% and the minimum was observed with 57% size reduction. The same pattern of variation was observed in the micro hardness study done by applying 100 g load. Hence, it is clear that increase in hardness from the cast specimens to hot-forged specimens is due to the closure of micro porosities as well as due to the grain refinement after hot forging.

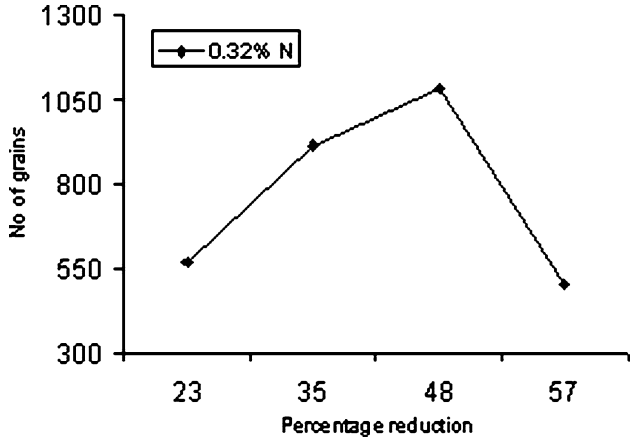

Fig. 6 % Reduction vs. no of grains/sqmm

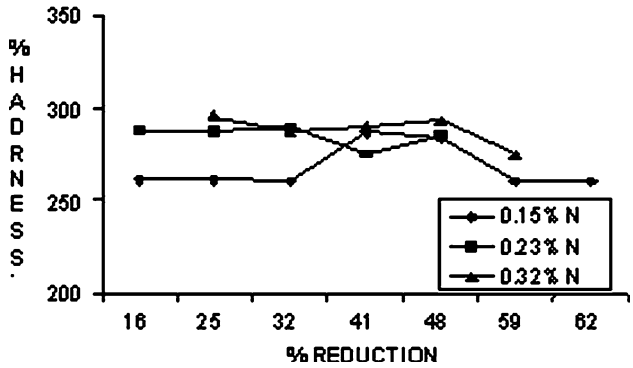

Fig. 7 % Reduction vs. hardness at 10 kg load

Additionally, the hardness values in all the reductions of 0.32% N alloy are higher compared to that of alloys with 0.15 and 0.23% N in hot-forged condition of similar size reduction (Fig. 7). This is due to the presence of higher-nitrogen content and the consequent higher-austenite volume.

3.3.3 Effect of Hot Forging on Impact Toughness. The effect of percentage deformation on impact strength of 0.32% N alloy is given in Table 4. The impact strength value of unforged specimen is 114 J. Impact strength of forged specimens range from 88 to 105 J. The maximum impact strength of 105 J at 48% reduction is due to the grain refinement. The conclusion is supported by fracture surface analysis carried out using SEM for both 48 and 57% reduced specimens with finer and coarser structure, respectively, as shown in Fig. 8 and 9. Moreover, the higher magnification of the same 48% reduced specimen reveals dimple structure compared to the structure of 23% reduced impact specimens as shown in Fig. 10 and 11. The characteristics of fracture in 48% reduced specimen is fibrous with fine-grained aggregates at the center, which occupies less than 15% with shear lips from 8.1 to 10 mm. The characteristics of fracture in 57% reduced specimen is fibrous with fine-grained aggregates at the center which occupy more than 33% of the entire fracture area with shear lips from 5.1 to 8.0 mm. This observation made as per СЕП-2 (Russian standard), reveals that 48% reduced specimen is tougher than the 57% reduced specimen.

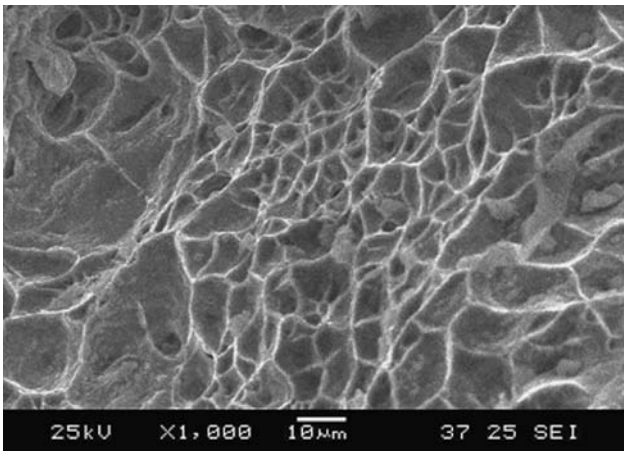

Fig. 8 SEM photograph of DSS alloy (room temperature fracture surface of 48% reduction—fine structure)

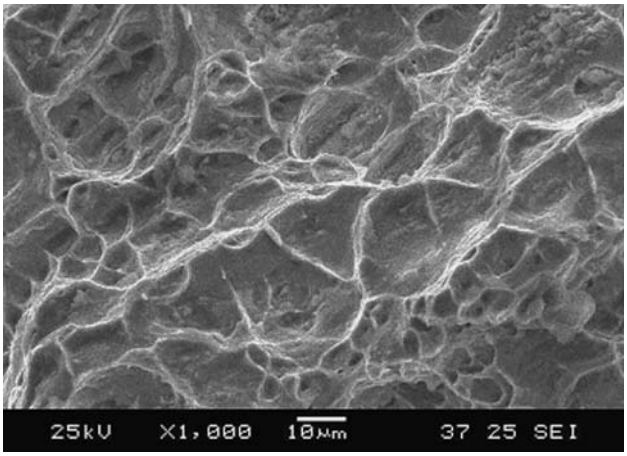

Fig. 9 SEM photograph of DSS alloy (room temperature fracture surface of 57% reduction—coarse structure)

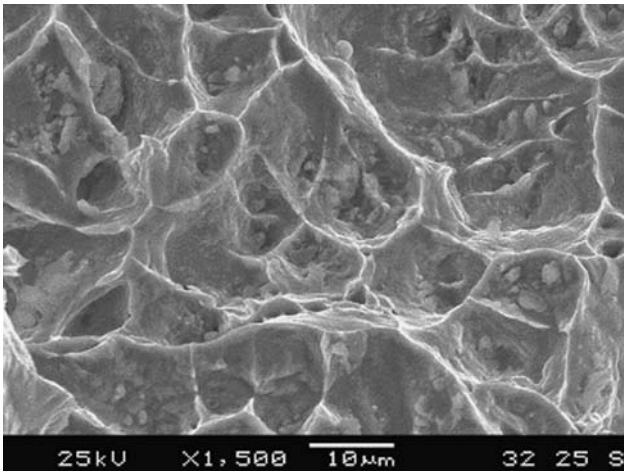

Fig. 10 SEM photograph of DSS alloy (room temperature fracture surface of 23% reduction—less dimple)

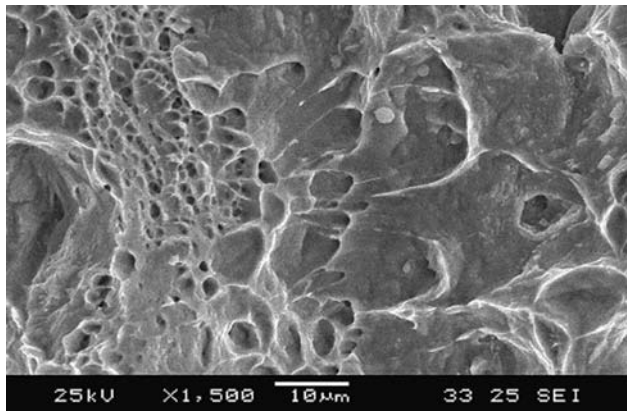

Fig. 11 SEM photograph of DSS alloy (room temperature fracture surface of 48% reduction—more dimple)

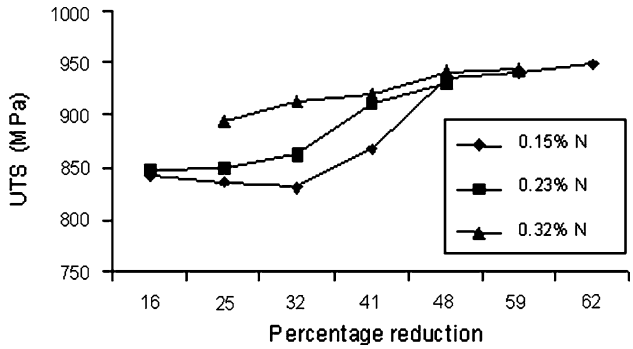

Fig. 12 % Reduction vs. UTS

The polynomial multiple linear regression equation 2 is developed to correlate impact strength to the percentage size reduction

$$Y = -0.0038X^3 + 0.41X^2 - 13.77X + 236.16 \quad : \quad R = 0.85 \qquad \text{(Eq 2)}$$

where Y, impact strength (J); X, % reduction; R, correlation coefficient

3.3.4 Effect of Hot Forging on Ultimate Tensile Strength (UTS) and Yield Strength. The effect of various size reductions of the 0.32% N alloy on the UTS and yield strength is given in Table 4. The UTS and yield strength of the unforged specimens are 789 and 597 MPa, respectively. While, a remarkable improvement in the UTS is noticed in all the hot-forged specimens, there is no comparative improvement in yield strength as a consequence of forging. As the % reduction increases from 23 to 57, ultimate tensile strength increases linearly from 894 to 943 MPa. It is also observed that the tensile strength values of alloy with 0.32% N are higher in all the size reductions when compared to that of alloys with 0.15 and 0.23% N (Fig. 12). This is due to the presence of higher-nitrogen content. This is in agreement with Vedani Nicodemi et al. (Ref 24) that tensile property is dependent on the material composition (particularly nitrogen) and on the degree of mechanical working.

There is no improvement in yield strength after hot forging. Also, the yield strength in all the size reductions of alloy with 0.32% N remains lower compared to that of alloys with 0.15

and 0.23% N (Fig. 13). This is because of higher-austenite content in all the size reductions of alloy with 0.32% N when compared to that of alloys with 0.15 and 0.23% N. He et al. (Ref 25) have also reported that yield strength decreases with increasing volume fraction of austenite in hot-rolled bars of duplex stainless steels.

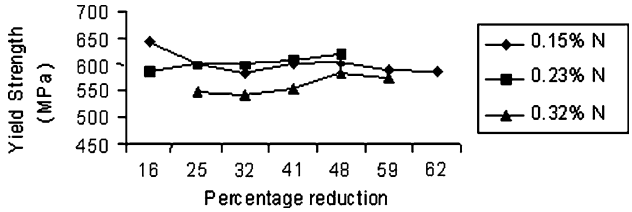

Fig. 13 % Reduction vs. yield strength

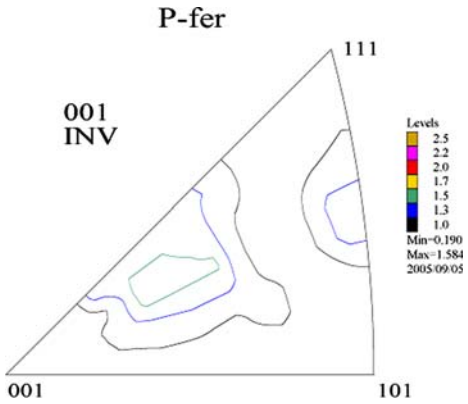

Fig. 14 IPF of ferrite phase in 48% reduced alloy with 0.32% N

The polynomial multiple linear regression equations 3 and 4 were developed to correlate UTS and Yield strength to the percentage size reduction:

$$Y = 1.546\,X + 859.748 \quad : \quad R = 0.95 \qquad \text{(Eq 3)}$$

$$Y = -0.009\,X^3 + 1.126\,X^2 - 42.153\,X + 1035.85 \quad : \quad R = 1 \qquad \text{(Eq 4)}$$

where Y, UTS and Yield strength in Eq 3 and 4 (MPa); X, % reduction.

3.3.5 Effect of Hot Forging on Grain Orientation. Specimen of 48% size reduction shows improved mechanical properties. Often, improvement in mechanical properties is caused by preferred orientation (texturing) of grains (Ref 6). Therefore texturing was studied using IPF and ODF to find out the relationship between grain orientation and improvement in mechanical properties.

Inverse Pole Figure (IPF) and orientation distribution function (ODF) for grains in the individual phases viz. ferrite and austenite, of alloy with 0.32% N are shown in Fig. 14-17. The contour plots drawn in the unit triangle shown in Fig. 14 reveals that the grains in the ferrite are not oriented at [001] [101] or [111] crystallographic direction. Instead, most of the grains tend to cluster about some particular orientation i.e., [112] [113] [115] [122]. The overall texturing or anisotropy is weak with maximum and minimum values intensity of 1.584 and 0.190, respectively. The texture of grains in ferrite along with crystal direction in alloy 3 is shown in Fig. 15. This ODF supports the Pole Figure showing low-intensity fibers running throughout the Euler space divided in sections of constant ϕ_2.

The contour plots drawn in the unit triangle shown in Fig. 16 reveals that a few grains in the austenite are oriented at [111] crystallographic direction. A few other grains are oriented

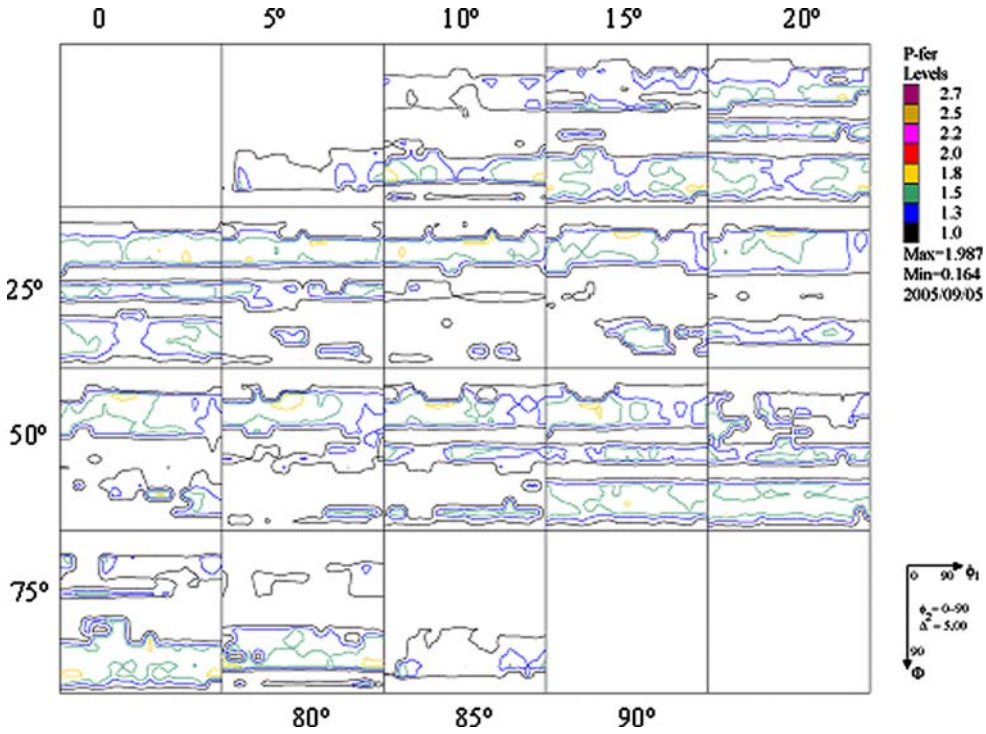

Fig. 15 ODF of ferrite phase in 48% reduced alloy with 0.32% N

at [113] [122] directions. When compared to the unit triangle of ferrite, the area of maximum intensity is higher in the unit triangle of austenite. This implies that texture formation is better in austenite when compared to ferrite. The texture of grains in austenite along with crystal direction of alloy 3 is shown in Fig. 17. This ODF supports the Pole Figure showing high-intensity fibers running throughout the Euler space divided in sections of constant ϕ_2. Austenite phase shows stronger texture as compared to ferrite grains for the same level of texturing. In general, texturing is weak in all the samples which indicate that the improved properties in 48% reduced samples are not due to preferred orientation.

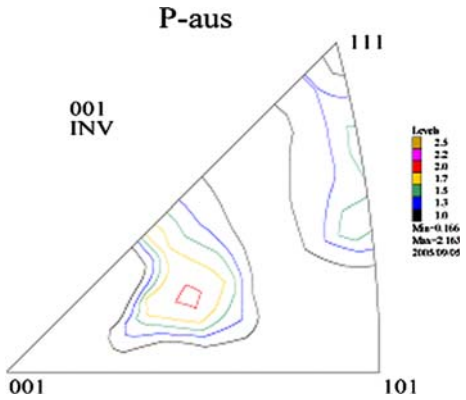

Fig. 16 IPF of austenite phase in 48% reduced alloy with 0.32% N

4. Conclusions

The following conclusions were drawn from the present work:

1. Micro porosities are observed in the as-cast material of DSS with 0.32% N, which leads to inferior mechanical properties.
2. Increase in the ferrite content is observed in all the size reductions after hot forging of the as-cast material.
3. Hot forged 0.32% N Duplex stainless steels show higher strength due to the increase in austenite content.
4. In the forged specimens of DSS with 0.32% N, the maximum hardness and maximum impact strengths are achieved in 48% size reduction compared to all other size reductions.
5. Grain refinement has contributed to the improvement in hardness and tensile strength of hot-forged specimen.
6. Fracture analysis for all the size reductions using SEM reveals ductile fracture with more dimple areas in 48% reduction and relatively more river type pattern in the remaining size reductions.
7. Fracture analysis for all the size reductions using SEM reveals fibrous characteristics with fine-grained aggregates at the center with shear lips from 5.1 to 10 mm.
8. Texture analysis of 48% reduced DSS alloy with 0.32% N, indicates that texturing is weak.
9. The improved mechanical properties in the hot-forged samples are attributable to grain refinement than texture formation.

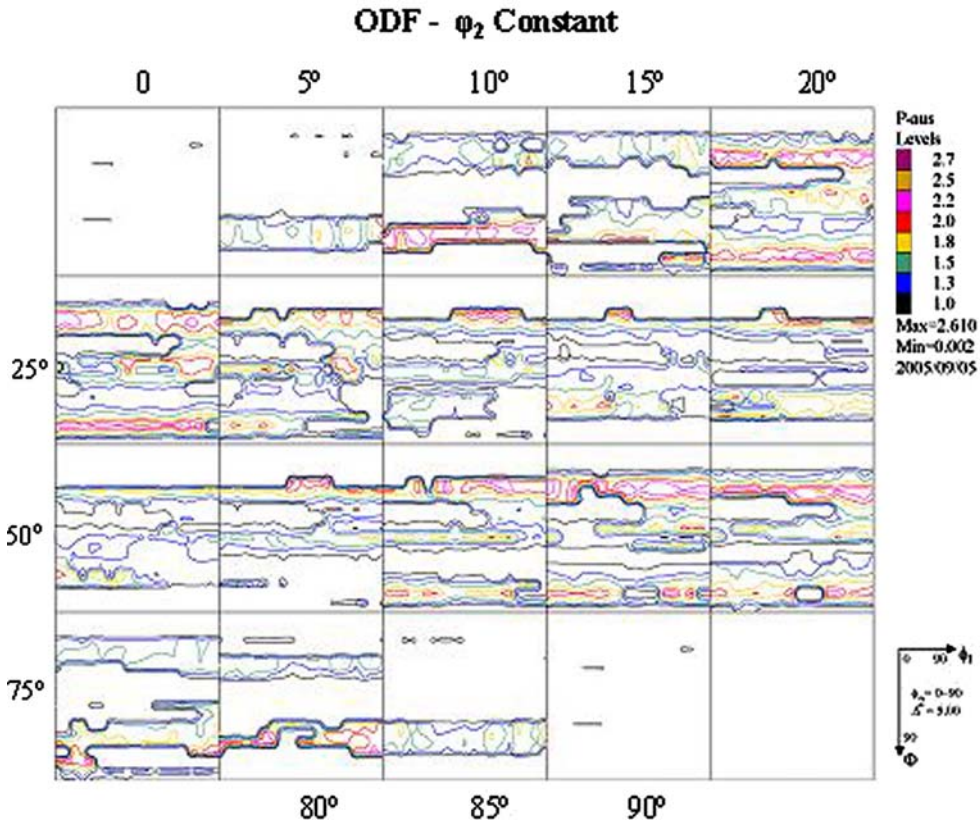

Fig. 17 ODF of austenite phase in 48% reduced alloy with 0.32% N

Acknowledgments

National Facility of Texture and Orientation Imaging Microscopy—Department of Science and Technology, India at IIT-Bombay, supported this work. The authors are grateful to M/s Auto Shell Co, m/s Commando engineers, Coimbatore for supplying and processing the DSS material. The authors are also thankful to Prof. Brindha and Prof. S.N. Mahalakshmi (Dept. of English, Sri Krishna College of Engg and Tech, Coimbatore, India) for their help in verifying the English grammar of this article.

References

1. J.R. Davis, *ASM Specialty Handbook-Stainless Steels*, ASM International, Materials Park, OH, 1996, ISBN: 0-87170-503-6
2. D.Y. Kobayashi and S. Wolynec, Evaluation of the Low Corrosion Resistant Phase formed during the Sigma Phase Precipitation in Duplex Stainless Steels, *Mater. Res.*, 1999, **2**(4), p 239–247
3. T. Millot, J.M. Dring, Corrieu, and La Maontagne, Influence of Heat Treatment on the Characteristics of X2 Cr Ni Mo N 25-07 Super Duplex Stainless Steel – Comparison of Two Heavy Section Pipes, *Proceedings of International Conference on Duplex Stainless Steels*, 1997, p 213–217
4. J.O. Nilson and A. Wilson, The Influence of Isothermal Phase Transformations on Toughness and Pitting Corrosion in the Super Duplex Stainless Steel SAF 2507, *Mater. Sci. Technol.*, 1993, **67**(5), p 545–554
5. V.G. Gavriljuk and H. Berns, *High Nitrogen Steels – Structure, Properties, Manufacture, Applications*, Springer, New York, 1997, ISBN 3-540-66411-4
6. J. Son, S. Kim, J. Lee, and B. Choi, Effect of N Addition on Tensile and Corrosion Behaviors of CD4MCU Cast Duplex Stainless Steels, *Metall. Mater. Trans. A*, 2003, **34A**, p 1617–1625
7. J.C. Lippold, I. Varol, and W.A. Baeslack, The Influence of Composition and Microstructure on the HAZ Toughness of Duplex Stainless Steels at −20 °C, III, *Welding J.*, 1994, **73**(4), p 75s–79s
8. Y.H. Park and Z.-H. Lee, The Effect of Nitrogen and Heat Treatment on the Microstructure and Tensile Properties of 25Cr-7Ni-1.5Mo-3W-xN DSS Castings, *Mater. Sci. Eng. A*, 2001, **297**, p 78–84
9. P. Chandramohan, S.S. Mohamed Nazirudeen, and R. Srivatsavan, The Effect of Nitrogen Solubility, Heat Treatment and Hot Forging on 0.15% N Duplex Stainless Steels, *Int. J. Mater. Prod. Technol. (IJMPT)*, 2006, **25**(4), p 281–296
10. R.N. Gunn, *Duplex Stainless steels-Microstructure, Properties and Applications*. Abington Publishing, Cambridge, England, 1997
11. F. Millet, J.-M. Pugnet, A. Franzi, B. Bonnefois, and J.-M. Lardon, New Proceedings Centrifugal Compressor in Super Duplex Stainless Steel, *Proceedings of International Conference on Duplex Stainless Steels*, 1997, p 713–722
12. T. Havn, A. Morini, H. Salbu, and O. Strandmyr, Quality Improvements on Duplex and Superduplex Cast and Forged Products for Offshore Applications: Producer and User View Points, *Proceedings of International Conference on Duplex Stainless Steels*, 1997, p 191–199
13. M.G. Mecozzi and M. Barteri, Effect of Alloying Elements and Impurity on Hot Ductility of 23% Cr 4% Ni Stainless Steel, *Proceedings of International Conference on Duplex Stainless Steels*, 1997, p 1011–1016
14. J. Charles, Super Duplex Stainless Steels: Structure and Properties, *Proceedings of International Conference on Duplex Stainless Steels*, Beaune, France, 1991, p 3–48
15. I. Samajdar, P. Ratchev, B. Verlinden, and E. Aernoudt, Hot Working of AA1050-Relating the Microstructural and Textural Developments, *Acta Mater.*, 2001, **49**(10), p 1759–1769
16. M. Kiran Kumar, I. Samajdar, N. Venkatramani, G.K. Dey, R. Tewari, D. Srivastava, and S. Banerjee, Explaining Absence of Texture Development in Cold Rolled Two-phase Zr-2.5 wt% Nb Alloy, *Acta Mater.*, 2003, **51**, p 625–624
17. J. Johannson and M. Oden, Load Sharing between Austenite and Ferrite in a Duplex Stainless Steel during Cyclic Loading, *Metall. Mater. Trans. A*, 2000, **31A**, p 1557–1570
18. J.J. Moveare and M. Oden, Influence of Elastic and Plastic Anisotropy on the Flow Behaviour in a Duplex Stainless Steels, *Metall. Mater. Trans. A*, 2002, **33A**, p 57–71
19. W. Horvath, W. Prantl, H. StroiBnigg, and E.A. Werner, Micro Hardness and Micro Structure of Austenite and Ferrite in Nitrogen Alloyed Duplex Stainless Steels between −20 and 500 °C, *Mater. Sci. Eng. A*, 1998, **256**, p 227–236
20. O. Balancin, W.A.M. Hoffman, and J.J. Jonas, Influence of Microstructure on the Flow Behaviour of Duplex Stainless Steels at High Temperatures, *Metall. Mater. Trans. A*, 2000, **31A**, p 1353–1364
21. G.S. Reis, A.M. Jorge Jr., and O. Balancin, Influence of the Microstructure of Duplex Stainless Steels on their Failure Characteristics During Hot Deformation, *Mater. Res.*, 2000, **3**(2), p 31–35
22. J.A. Jimenez, F. Carreno, O.A. Ruano, and M. Carsi, High Temperature Mechanical Behaviour of δ-γ Stainless Steel, *Mater. Sci. Technol.*, 1999, **15**, p 127–131
23. F.E. Al Jouni and C.M. Sellars, Recrystallisation after Hot Deformation of Two Phase Stainless Steels, *Mater. Sci. Technol.*, 2003, **19**, p 1311–1320
24. M. Vedani Nicodemi, E. Gariboldi, W. Nicodemi, and R. Roberti, Centrifugally Cast and Cold Worked Duplex and Superduplex Stainless Steel Pipes, *Proceedings of International Conference on Duplex Stainless Steels*, 1997, p 245–254
25. J. He, G. Han, S. Fukuyama, and K. Yokagawa, Tensile Behaviour of Duplex Stainless Steel at Low Temperatures, *Mater. Sci. Technol.*, 1999, **15**, p 909–919